

Received December 24, 2018, accepted January 10, 2019, date of publication January 23, 2019, date of current version February 8, 2019.

Digital Object Identifier 10.1109/ACCESS.2019.2894342

A Novel Inertia Identification Method and Its Application in PI Controllers of PMSM Drives

KAI LIU^{ID}, CHUANG HOU, AND WEI HUA^{ID}, (Senior Member, IEEE)

School of Electrical Engineering, Southeast University, Nanjing 210096, China

Corresponding author: Wei Hua (huawei1978@seu.edu.cn)

This work was supported in part by the National Key Research and Development Programme of China under Grant 2017YFB1300900, and in part by the National Natural Science Foundation of China under Grant 51777032.

ABSTRACT A novel method for inertia determination of a permanent magnet synchronous machine (PMSM) drive is proposed and analyzed, which employs a sinusoidal perturbation torque with a dc offset to drive the PMSM, and the amplitudes of reference sinusoidal torque and sinusoidal speed response are used to compute the system inertia. Compared with other methods, it is robust and fast to obtain the accurate quantity of the inertia. First, the inverter measures the resistances and inductances of a PMSM through a static voltage vector and stand-still frequency response experiments. The parameters are adopted to design the current proportion and integral controller and make both dq-axes currents to perform the first-order response. Second, the results of constant torque experiment employing the current controller are applied to get the friction coefficient and no-load torque. Third, a sinusoidal torque with a dc offset is applied and the response performs a sinusoidal speed with a constant offset. All the above experimental results and other preinstalled parameters are employed to get the system inertia, and the accuracy is verified by another experiment. As compensation for a position signal from a hall sensor, a corresponding method is also proposed to compute the sinusoidal speed response amplitude, which is the key in the procedure.

INDEX TERMS Inertia identification, sinusoidal motion torque with offset, first-order response, position hall sensor, PMSM.

I. INTRODUCTION

Recently, the developments of power electronics and permanent magnet synchronous machines (PMSMs) make PMSM-based drive system more and more popular. Proportion and integral (PI) regulator is widely applied in the occasions where the requirements for control performance are not so demanding. Generally, detailed and precise parameters information of a PMSM-drive system is of vital importance for the design of a PI controller or any other controllers [1]–[7], [23]–[26]. Electrical parameters, such as resistances and inductances of armature windings, are easy to measure by respective tools and methods (Resistance can be measured by an electric bridge and dq-axes inductances by Stand-Still Frequency Response (SSFR) experiments [8]). Since the relationship between steady speed and electromagnetic torque performs a linear function, the friction coefficient and no-load torque can be measured by a constant torque experiment that will be introduced later. In addition to the mentioned parameters, the inertia of the whole drive system including the PMSM and the load is so important for speed control loop design, meanwhile it is usually difficult to measure.

Numerous efforts have been made to try to get a precise identification of the inertia [3], [5], [7], [9]–[20], [23]–[26]. Among them, there is a very simple and convenient one where the curve of speed acceleration or deceleration is regarded as a straight line. With this assumption, the inertia can be calculated using the slope of the speed curve recorded by a controller [9]. Definitely, the method based on the speed curve is a good way, especially for the applications where the accuracy of control is not so strict.

For some high-precision control applications, a method based on disturbance observer which employs the orthogonal relation among the torque components of the estimated disturbance torque to get real torque values is presented in [5], [10], and [11]. This method requires a series of complex procedures, but the accuracy and robustness are very good. It is necessary to point out that the procedure of integral in this method is time-consuming and the observer pole needs detailed design, which will consume much time, too. The inertia measurement is the first step for a PMSM controller design, and the design procedure of the observer should be simple and fast. In addition, the pole of the observer that is used to measure inertia in this method needs to be

calculated for each motor system individually, and a common way is unavailable. Obviously, it will complicate the design procedure of the controller. On the other hand, all the other observers, such as model reference adaptive system (MRAS) [7], [12], [13], full-order state observer [14], Extended Kalman Filter [15], etc., have to face the same problems those exist in [10], namely detailed pole design and complicated procedures.

Recursive least square (RLS) method is another method for inertia measurement, which employs the acceleration or deceleration process to finish a RLS analysis, and then the inertia value can be obtained [16]–[18]. The noise suppression and successful convergence to the actual inertia value can be assured in the RLS method. However, the measurement process requires the motor to be controlled in a steady state in advance. If the motor parameters cannot be predetermined, it will take lots of time to tune parameters of the controller. Also, the procedure of the product development will be slowed down, as the foregoing mentioned.

In addition, a fast inertia measurement method is proposed recently, where a sinusoidal torque is applied to drive the testing motor [19]. The phase angle of the sinusoidal torque can be caught when the speed is zero. If no-load torque can be neglected, the friction torque component and the inertia torque component in the motion equation will perform an orthogonal relationship, which can be used to calculate the inertia. This method is very fast and has an excellent adaption for most occasions because it employs the basic motion equation rather than observers. Therefore, it barely needs few tuning procedures. But the condition that this method works well is that the no-load torque should be small enough when compared to the motion torque and friction torque. However, when the no-load torque cannot be ignored, this method does not work well. For example, if the motor is used to motivate a robot arm, the no-load torque includes a considerably non-negligible component, which comes from the gravity of the products lifted by the robot arm.

In [10] and [19], periodical signals were employed to obtain the inertia, but they face some difficulties, i.e. complex data processing, non-commonalities, and too much time of tuning. In order to address these problems, in this paper a novel method is proposed for these special occasions with the features of decreasing complexities and increasing robustness, based on the method of periodical actuation coming from [10] and [19]. A periodically sinusoidal electromagnetic torque with a dc offset is used to drive the tested motor, and the relationship between the amplitudes of sinusoidal torque and sinusoidal speed response is utilized to get the inertia value. It can avoid the problem of “no-load torque” that exists in [19] and the problem of complex integral process that exists in [10]. In addition, this method requires no observers and consequently, no tuning procedures.

This paper is organized as follows. Firstly, the basic principles of the proposed method are derived in section II. Then, the design of current loop and the measuring of parameters except for the inertia value are realized in section III.

Thereafter, in section IV the inertia is measured by the method proposed in section II and its accuracy is verified based on classical automation control theory. Especially, for some special occasions where a low-precision hall sensor is equipped into the PMSMs, a method for computing the sinusoidal speed amplitude that plays a key role in the procedure of inertia measuring is presented in section V. Finally, conclusion is given in section VI.

II. CONCEPT OF THE NEW INERTIA IDENTIFICATION METHOD

The motion equation of a PMSM-based drive system is given as:

$$T_e - T_l = J \frac{d\omega_m}{dt} + B\omega_m \quad (1)$$

where, T_e is the electromagnetic torque produced by the interaction between the open-circuit air-gap PM flux-density due to magnets and the synthesized armature reaction due to armature winding currents; B is the friction coefficient; T_l is the no-load torque due to cogging torque, friction between the shaft and the bearing, etc.; and J is the inertia of the whole system including the inertias of the PMSM itself and the coupling load rotating synchronously. Equation (1) is a first-order homogeneous linear differential equation, where $T_e - T_l$ is defined as motion torque. There are three unknown parameters in this equation, namely, T_l , J , and B .

It's supposed that $T_e - T_l = T_0 \cos(\omega t)$, thus equation (1) can be rewritten as:

$$T_0 \cos(\omega t) = J \frac{d\omega_m}{dt} + B\omega_m \quad (2)$$

where T_0 is the amplitude of the motion torque, which satisfies a pure sinusoidal distribution with an angle frequency of ω .

Applying Laplace Transform to equation (2), the speed response can be expressed concisely as:

$$\omega_m(s) = \frac{T_0 s}{(s^2 + \omega^2)((sJ + B))} \quad (3)$$

It is supposed that $\omega_m = 0$ when $t = 0$. If $T_e - T_l = T_0 \cos(\omega t)$, the speed response of the PMSM turns out to be

$$\omega_m(t) = \frac{T_0}{\sqrt{(B^2 + J^2\omega^2)}} \cos(\omega t - \beta) + \frac{T_0 B}{B^2 + J^2\omega^2} e^{-\frac{B}{J}t} \quad (4)$$

The first term of equation (4) is a sinusoidal speed response and the second term is a transient response that will disappear after several time constants. Obviously, with the disappearance of the second term, the inertia can be computed by two paths, one from the sinusoidal speed amplitude ω_0 which is $T_0/\sqrt{B^2 + (J\omega)^2}$ in equation (4), and the other from the phase angle β of the steady state response of speed. The two paths will be analyzed in sub-sections A and B as follows.

A. BASED ON PHASE ANGLE β

From equation (4), it can be found that the phase angle β is equal to $\arctan(\omega J/B)$, where B can be achieved from the constant electromagnetic torque experiment. So, J can be computed if β that is phase angle delay between two sinusoidal signals is known. The phase-locked technology can be applied to get the phase shift β . However, the speed needs to be measured precisely at any instant using this technology. Generally, when the motor is equipped with a resolver or a photoelectric encoder which have a resolution higher than 1024, the speed signal is precise enough to be applied in the computation of the phase delay. However, some motor drive systems only have a hall sensor for rotor positions with very low precision, which cannot instantly offer a precise speed signal. Besides, the computing process using the delay angle β needs a step of arctangent computation which is very time-consuming. Therefore, the method based on β to compute inertia is not a practical choice.

B. BASED ON SINUSOIDAL SPEED AMPLITUDE

The sinusoidal speed amplitude can also be used to compute the inertia since the steady sinusoidal speed amplitude is easy to measure by an encoder or a resolver using Fast Fourier Transform [21]. Under circumstances where the position sensor is a hall sensor, a precise speed amplitude computing method is proposed and will be presented in section IV.

According to equation (4), the inertia can be expressed as:

$$J = \frac{\sqrt{\left(\frac{T_0}{|\omega_0|}\right)^2 - B^2}}{\omega} \tag{5}$$

where ω_0 is the amplitude of sinusoidal speed response under a sinusoidal motion torque, namely $T_e - T_l = T_0 \cos(\omega t)$. If the speed amplitude can be measured precisely, the inertia can be computed by equation (5) since all other parameters have been predetermined.

As foregoing analyzed, it is required that $T_e - T_l = T_0 \cos(\omega t)$. However, T_l will reverse its polarity and consequently, the sign as the speed sign changes. Therefore, the real electromagnetic torque should be set as:

$$T_e = \begin{cases} |T_l| + T_0 \sin(\omega t), & \text{when } \omega_m < 0 \\ -|T_l| + T_0 \sin(\omega t), & \text{when } \omega_m > 0 \end{cases} \tag{6}$$

Fig. 1 illustrates an approximate relationship among electromagnetic torque T_e (the bold red line), motion torque $T_e - T_l$ (the thin golden line), speed response ω_m (the dashed black line), and no-load torque T_l (the dotted blue line). It can be seen that due to the sign reversion of the no-load torque versus the speed sign, the resultant electromagnetic torque cannot be continuously produced if an ideally sinusoidal speed response is desired.

If $T_e - T_l = T_0 \cos(\omega t)$ is applied, T_e needs to be produced as the bold red line in Fig. 1, which means the electromagnetic torque needs a double T_l variation in a very short time. Therefore, the current flowing into the armature winding needs

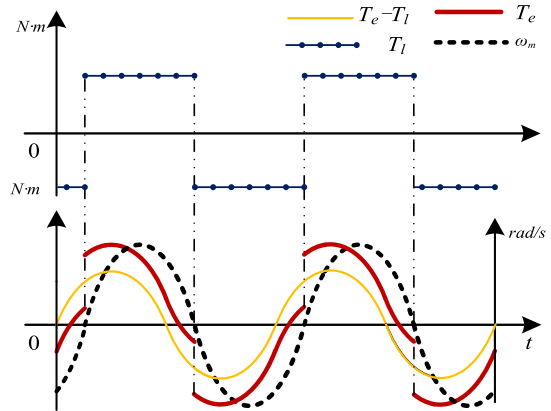


FIGURE 1. Sinusoidal speed response due to corresponding motion torque, electromagnetic torque, and no-load torque waveforms.

to change very fast. However, it is almost impossible for an inverter-fed PMSM drive system, since although the electrical time constant is far less than the mechanical motion time constant, the required current change needs the inverter equipped with a considerably large capacitance. Another problem is that the instant is very hard to be caught when the speed is equal to zero, which can be found in [19]. Therefore, it is not an optimal solution, either.

According to the problems analyzed above, this paper proposes a new method that applies a sinusoidal electromagnetic torque with a dc offset component to drive the motor, where from the blending speed response, the inertia can be computed easily.

The basic concept of the proposed new method is introduced as follows. The discontinuity of ideal electromagnetic torque comes from the changeable speed sign. If the speed sign remains positive, the sign of no-load torque will be unchangeable. Considering the motion system is a linear system, we recognize that if a sinusoidal electromagnetic torque with a dc offset is applied to drive the motor, the speed response should be a sinusoidal response with a dc offset, as long as the sum response is not less than zero. And this can be assured only if the dc offset torque T_{dc} is larger than the no-load torque T_l . Finally, in this way, two electromagnetic torque components (one sinusoidal component and one dc offset component) and the respective speed response can be separated. The detailed computation is as follows.

The modified motion equation is rewritten as:

$$T_{dc} + T_0 \cos(\omega t) = J \frac{d\omega_m}{dt} + B\omega_m + T_l \tag{7}$$

Since the response of only a sinusoidal electromagnetic torque component is obtained in equation (4), the calculation of the speed response due to the dc offset torque is given by:

$$T_{dc} = J \frac{d\omega_{mdc}}{dt} + B\omega_{mdc} + T_l \tag{8}$$

where ω_{mdc} is the speed response of offset dc torque.

Based on the superposition theorem, the speed response due to the dc torque component ω_{mdc} can be expressed as:

$$\omega_{mdc}(t) = \frac{T_{dc} - T_l}{B} - \frac{T_{dc} - T_l}{B} e^{-\frac{B}{J}t} \quad (9)$$

Hence, the whole speed response can be expressed as:

$$\omega_m(t) = \frac{T_0}{\sqrt{(B^2 + J^2\omega^2)}} \sin(\omega t - \beta) + \frac{T_0 B}{B^2 + J^2\omega^2} e^{-\frac{B}{J}t} + \frac{T_{dc} - T_l}{B} - \frac{T_{dc} - T_l}{B} e^{-\frac{B}{J}t} \quad (10)$$

When several mechanical time constants pass, these two transient terms in equation (10) will disappear, and the final steady speed response can be derived as:

$$\omega_{mdc}(t) = \frac{T_0 B}{\sqrt{(B^2 + J^2\omega^2)}} \sin(\omega t - \beta) + \frac{T_{dc} - T_l}{B} \quad (11)$$

From equation (11), it can be found that the final speed response includes a sinusoidal speed component and a constant speed component. Consequently, the inertia can be computed from the sinusoidal speed response as presented above. The approximated relationship between the electromagnetic torque and the speed response is shown in Fig. 2.

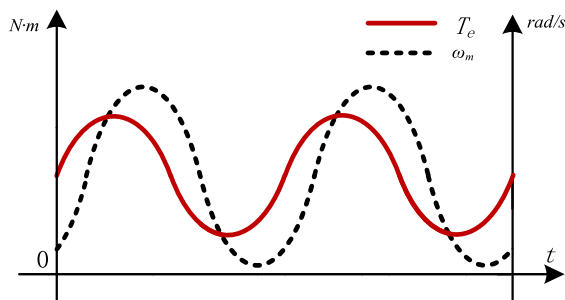


FIGURE 2. Speed response and electromagnetic torque with a constant torque offset.

III. CURRENT LOOP TUNING AND PARAMETERS MEASUREMENTS

This section will present the detailed concept and the implementation process of the proposed new method based on combined electromagnetic torque, which is composed of a sinusoidal torque component and a dc torque offset. The method requires the motor to produce the actual electromagnetic torque tracking the referenced torque signal. To achieve this goal, a PI current controller is normally functioned as an electromagnetic torque controller. Although there are some disadvantages with the PI current controller, it's still widely used. There are many techniques to tune the parameters of the PI controller. Since the measurement of inertia only needs an electromagnetic torque controller, and all electrical parameters can be measured, the parameters of a PI current controller can be designed by dq -axes frame and classical control theories.

Equations (12) and (13) are the voltages equations in dq -axes frame of a PMSM.

$$U_d = L_d \frac{di_d}{dt} - \omega_e L_q i_q + r i_d \quad (12)$$

$$U_q = L_q \frac{di_q}{dt} + \omega_e L_d i_d + \omega_e \psi_m + r i_q \quad (13)$$

where, U_d/U_q , i_d/i_q , L_d/L_q are the voltages, armature currents, winding inductances in the dq -axes, respectively; ψ_m , ω_e , and r is the d -axis PM flux-linkage, electrical angle frequency (rad/s), and armature resistance per phase, respectively.

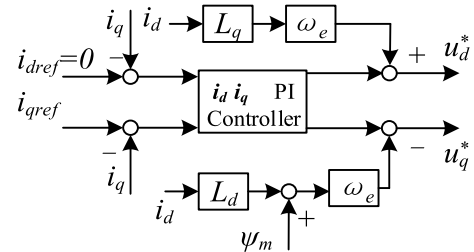


FIGURE 3. The basic scheme of vector control loop for a PMSM.

Fig. 3 illustrates the basic principle of vector control for a PMSM. With the measured speed, the d - and q -axis voltage compensations can be accomplished by adding the components of $\omega_e L_q i_q$ and $-\omega_e(L_d i_d + \psi_m)$ to d - and q -axis current PI controller outputs, respectively. After the compensation, equations (12) and (13) can be simplified as

$$U_{do} = L_d \frac{di_d}{dt} + r i_d \quad (14)$$

$$U_{qo} = L_q \frac{di_q}{dt} + r i_q \quad (15)$$

where U_{do} and U_{qo} are the combined dq -axes voltages existing in the winding inductance and resistance, respectively.

Based on equations (14) and (15), it can be seen that the dq -axes current responses can be designed as a first-order response. However, the inverter power devices delay and the sampling delay demand specific attentions to the design of a PI current controller. Under different circumstances, different methods should be adopted, and the key judgment rule is whether both the delays as a result of inverter and sampling can be neglected compared with the system bandwidth. When the delays can be neglected, method A will be chosen, otherwise, method B.

A. DESIGN OF CURRENT LOOP PARAMETERS WITHOUT DELAYS

When the delays are small enough compared to the system control bandwidth, the current loop is illustrated in Fig. 4.

After compensation, the transfer function of dq -axes current responses can be deduced as:

$$\frac{i_d(s)}{U_{do}(s)} = \frac{\frac{1}{r}}{\left(1 + \frac{sL_d}{r}\right)} \quad (16)$$

$$\frac{i_q(s)}{U_{qo}(s)} = \frac{\frac{1}{r}}{\left(1 + \frac{sL_q}{r}\right)} \quad (17)$$

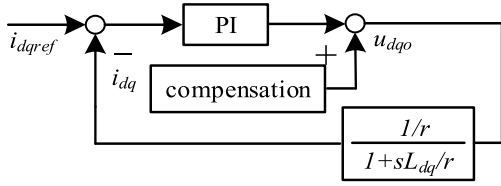


FIGURE 4. Current loop under compensation without considering delays.

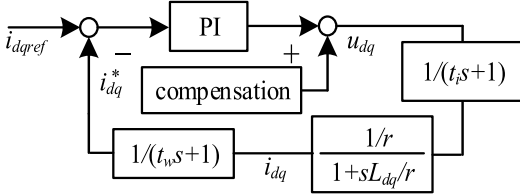


FIGURE 5. Current loop under compensation considering delays.

From the PI control loop scheme in Fig. 4, the open loop function can be figured out as:

$$PI(s) \frac{i_{dq}(s)}{U_{dqo}(s)} = \frac{k_{ip}k_{ii}(1+s/k_{ii})}{s} \frac{1/r}{(1+sL_{dq}/r)} \quad (18)$$

where, k_{ip} is proportional coefficient, k_{ii} is integral coefficient, and i_{dq} , u_{dqo} , L_{dq} are dq -axes currents, combined dq -axes voltages, and dq -axes inductances, respectively.

Obviously, the open loop transfer function includes a zero and a pole. Thus, it can be simplified to

$$PI(s) \frac{i_{dq}(s)}{U_{dqo}(s)} = \frac{k_{ip}k_{ii}}{s} \frac{1}{r} \quad (19)$$

under $1+s/k_{ii} = 1+sL_{dq}/r$ and $k_{ii} = r/L_{dq}$, and the closed loop function is described as:

$$\frac{i_{dq}(s)}{i_{dqref}(s)} = \frac{1}{\frac{L_{dq}}{k_{ip}}s + 1} \quad (20)$$

According to equation (20), the current loop can be designed as a first-order response, and $\omega_{ci} = k_{ip}/L_{dq}$ is satisfied. The system bandwidth can be designed using k_{ip} . Additionally, it should be noted that the maximum value of ω_{ci} is limited by DC voltage and protection requirements.

B. DESIGN OF CURRENT LOOP PARAMETERS CONSIDERING DELAYS

When the delays, including the inverter delay t_i and the current sampling delay t_w , cannot be ignored, the modified current loop design considering delays is depicted as Fig. 5.

Taking these two delays into consideration, the open loop transfer function is given as:

$$G(s) = \frac{k_{ip}k_{ii}(1+s/k_{ii})}{s} \frac{1/r}{(1+sL_{dq}/r)} \frac{1}{(t_i s + 1)} \quad (21)$$

The feedback function is

$$H(s) = \frac{1}{(t_w s + 1)} \quad (22)$$

Similar to method A, k_{ii} is set as r/L_{dq} . When k_{ii} is determined, the current close loop transfer function is expressed as:

$$\frac{i_{dq}(s)}{i_{dqref}(s)} = \frac{(k_{ip}/L_{dq})(t_w s + 1)}{(k_{ip}/L_{dq}) + s(t_w s + 1)(t_i s + 1)} \quad (23)$$

In equation (23), $(t_w s + 1)(t_i s + 1)$ can be simplified to $(t_{sum} s + 1)$, where $t_{sum} = t_i + t_w$. In Fig. 5, there is only a first-order delay between i_{dq} and i^*_{dq} , and the delay is small enough that the difference between these two signals can be neglected in the current response. For the design convenience, i^*_{dq} can be used as the torque response instead of i_{dq} . Therefore, (23) is transformed as:

$$\frac{i^*_{dq}(s)}{i_{dqref}(s)} = \frac{1}{t_{sum} \frac{L_{dq}}{k_{ip}} s + \frac{L_{dq}}{k_{ip}} s + 1} \quad (24)$$

Equation (24) is a second-order homogeneous system. According to basic control theory, to keep the response steady and fast, the damp is set as $\sqrt{2}$, and k_{ip} should be $L_{dq}/(2t_{sum})$.

Whether to use a second-order system or not depends on the comparison between the delay length and the motor electrical time constant. But a practical method is implemented as follows:

- (1) Setting r/L_{dq} for k_{ii} , and one tenth of $L_{dq}/(2t_{sum})$ for k_{ip} .
- (2) Increasing the value of k_{ip} gradually, meanwhile observing a step signal response of current loop until a vibration appears.
- (3) The final k_{ip} can be adjusted based on the value of k_{ip} in step (2) according to the response requirements of the motor drive system.

This method is used by authors in many PMSM controllers, and it always performs well.

C. ELECTRICAL PARAMETERS MEASUREMENTS

The current loop design has been previously introduced including two cases, namely with and without considerations of the influence of delays. The necessary electrical parameters used in the inertia identification procedure, such as the resistance per phase and dq -axes winding inductances, are to be measured.

To acquire the phase resistances of a PMSM, the simplest way is to use a universal meter. However, for a practical PMSM-based drive system, in addition to the winding resistances from the machine itself, the resistances due to the switched-on IGBTs should also be considered since the voltage vector is based the duty of pulse width modulation (PWM) and the DC voltage quantity [21], [22].

Hence, a static voltage vector (SVV) technology to get the real resistance based on space vector pulse width modulation (SVPWM) is proposed, where SVV means the angle of the voltage vector is maintained with a constant quantity, and then the voltage vector length is adjusted. Thus, the voltage vector divided by the current vector is the resistance quantity and the experiment can be carried on many different angles

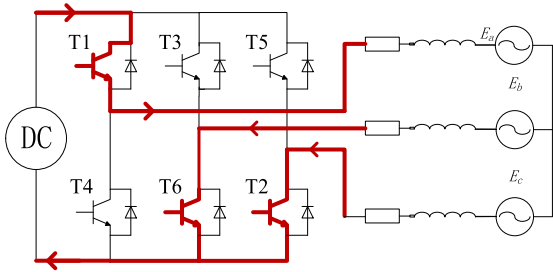


FIGURE 6. The current directions and paths in a SVV method.

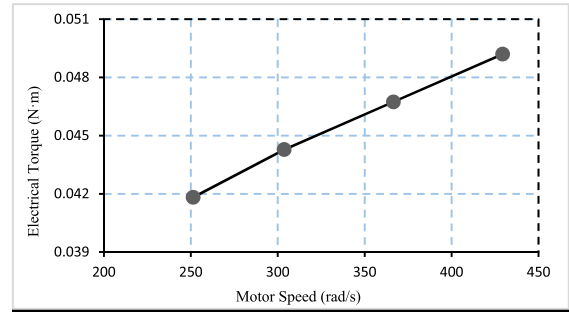


FIGURE 8. Constant electromagnetic torque motor speed vs electromagnetic torque.

TABLE 1. Key electric specifications of the PMSM.

Parameters	Value
Resistance (R_s)	0.41 Ω
d -axis inductance (L_d)	0.403 mH
q -axis inductance (L_q)	0.403 mH
PM flux linkage (ψ_m)	8.199 mWb
Friction coefficient	4.145e-5N·m·s
No-load torque	0.0316N·m

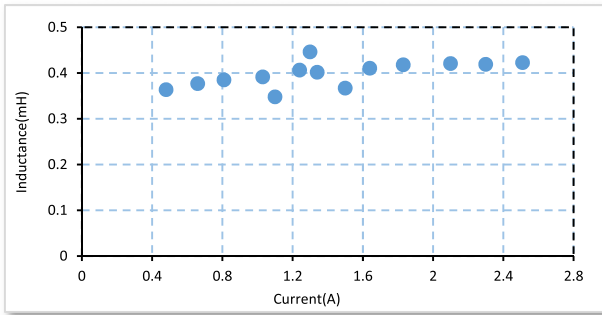


FIGURE 7. The measured dq-axes inductances of the PMSM by SSFR.

of the voltage vector considering many statuses of IGBTs. The final result can be a mean value using different voltage vector lengths and angles. The experimental result of the phase resistance of the PMSM-based system discussed in this paper is about 0.41 Ω . Fig. 6 illustrates a current-flowing chart of a static voltage vector with an angle of zero degree.

Stand still frequency response (SSFR) method is used to obtain the quantities of dq -axes inductances [8]. If the tested motor doesn't rotate, namely ω_e is zero, equations (12) and (13) are simplified as:

$$U_d = L_d \frac{di_d}{dt} + ri_d \tag{25}$$

$$U_q = L_q \frac{di_q}{dt} + ri_d \tag{26}$$

Moreover, if U_d is a sinusoidal quantity, i_d should be a sinusoidal response, and that works at q -axis current as well.

It is well-known that the surface-mounted PMSM satisfies $L_d = L_q$. Therefore, it is not necessary to separate i_d and i_q . Let the inverter output a circled voltage vector, so equations (25) and (26) can be seen as a circuit composed of an inductor in series with a resistor. With this simplified model, L_d and L_q are easy to be computed. The experimental results are shown in Fig. 7. Even the applied amplitudes of the injected armature current vectors are different, the measured inductance quantities keep an almost stable value of 0.40mH with acceptable variations.

D. MECHANICAL PARAMETERS MEASUREMENTS

Apart from the motor inertia J , the friction coefficient B and the no-load torque T_l are unknown. In part A and part B, a stable current controller is designed. Let the controller output

different i_q , and the steady speeds at different i_q are recorded. Meanwhile, the output torque of the motor with different i_q can be calculated by

$$T_e = \frac{3}{2}p\psi_m i_q \tag{27}$$

where p is the pole pairs of the motor and ψ_m is PM flux linkage coming from back-EMF experiment.

The constant electromagnetic torque experimental results are shown in Fig. 8, where the speed and the electromagnetic torque perform as a linear function, which agrees well with theoretical analysis. Due to the excellent linearity of the curve, it is unnecessary to apply a complex fitting algorithm. Based on fitting result from Microsoft office excel, $T_e = 4.145e^{-5}\omega + 0.0316$, $B \approx 4.145e^{-5}N\cdot m\cdot s$, and $T_l \approx 0.0316N\cdot m$.

The key specifications of the tested PMSM is listed in Table 1.

IV. INERTIA IDENTIFICATION AND SPEED LOOP EXPERIMENTS

Based on the acquisitions of parameters as presented in Tab. 1 in Section III, the implementation and verification of the proposed new inertia identification method will be conducted in this section.

Fig. 9 is the experiment platform for a 60W PMSM drive. The motor platform consists of four parts, including the load motor, the PMSM, the position sensor, and the controller. The load machine is a DC motor whose power rating is 100W. There are two position sensors, i.e., a hall sensor equipped into the PMSM and a photoelectric encoder in the right part of the platform.

According to sections II and III, the inertia measuring experiment can be performed by a universal AC motor

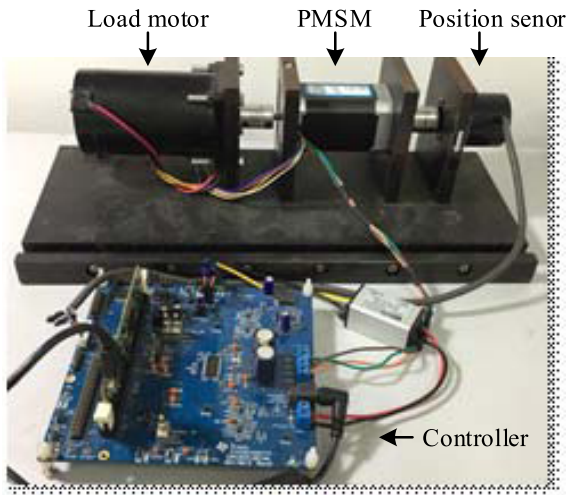


FIGURE 9. The experiment platform for the PMSM drive system.

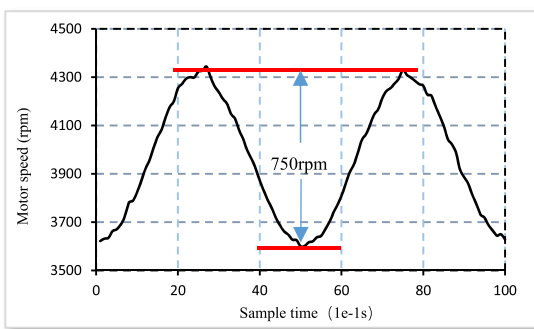


FIGURE 10. The speed response of the PMSM with $i_q = 1 + 0.6\sin(2\pi t)(A)$.

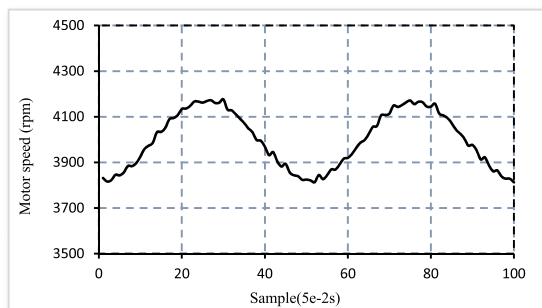


FIGURE 11. The speed response of the PMSM with $i_q = 1 + 0.6\sin(4\pi t)(A)$.

controller. The q -axis reference current is composed of a sinusoidal current component and a dc current offset. The q -axis current amplitude should not be too small to be accurately measured, and the maximum value of q -axis current should be limited by DC voltage and protection requirements. The q -axis current is controlled as $i_q = 1 + 0.6\sin(2\pi t)(A)$, and the resultant sinusoidal speed amplitude is about 750rpm, as shown in Fig. 10. Consequently, according to equation (5), the calculated inertia is about $J = 1.227e^{-4} \text{ kg}\cdot\text{m}^2$. Another experiment is conducted using $i_q = 1 + 0.6\sin(4\pi t)(A)$, and the speed response is shown in Fig. 11, where the corresponding inertia $J = 1.231e^{-4} \text{ kg}\cdot\text{m}^2$.

Further, randomly varying amplitude and frequency of the sinusoidal torque in an appropriate range where the motor can work smoothly and the experimental results are shown in Fig. 12. As can be seen, the result varies slightly, which verifies the robustness of the proposed inertia identification method.

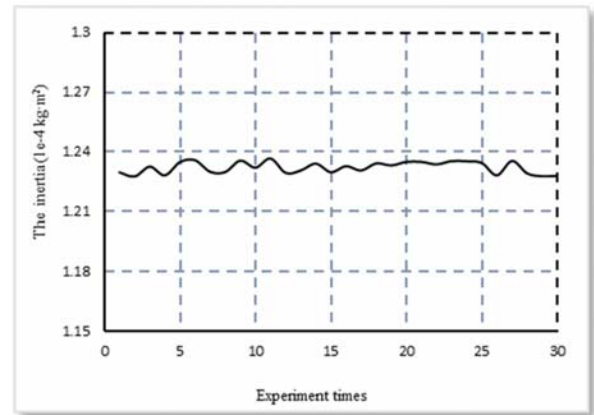


FIGURE 12. The calculated inertia under random experiment conditions.

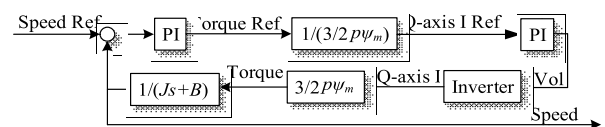


FIGURE 13. The PMSM-based control scheme for speed loop design and inertia accuracy verification.

To evaluate the accuracy of the inertia measured by the method above, a speed PI controller is employed to realize a first-order speed response, and the control principle is showed in Fig. 13.

Considering the first-order speed response under a step signal is very hard to record and analyze, we let the input signal of the first-order system perform as a sinusoidal quantity with a dc offset. The cut-off frequency of the first-order system is set the same as the frequency of sinusoidal reference speed signal. If the resultant phase delay and speed amplitude ratio are 45 degrees and $\sqrt{2}$ respectively, it can be verified that the inertia measured using this method is precise and the speed controller design is correct completely.

For the first-order speed system response, all the parameters involved in the motion equation, i.e., the friction coefficient, the inertia of PMSM system, and the no-load torque, have been determined. Generally, the mechanical motion time constant of a PMSM system is far larger than the electrical time constant. For this PMSM system, J/B is much bigger than L_d/r or L_q/r . From the above experimental results, J/B is 2.96 and L/r is $1e^{-4}$. (The experimental motor is a surface-mounted PMSM, namely $L_d = L_q$. For convenience, we assume L stand for L_d or L_q .)

Under this condition, for speed loop design, the current loop can be equivalent to 1 in the transfer function for the whole system, and the speed open loop function can be

written as

$$G_{\omega}(s) = \frac{k_{op}k_{\omega i}(1 + s/k_{\omega i})}{s} \frac{1/B}{1 + sJ/B} \quad (28)$$

Just like the method in current loop design, and the speed open loop transfer function can be simplified as

$$G_{\omega}(s) = \frac{k_{op}}{Js} \quad (29)$$

with $k_{\omega i} = B/J$. The system transfer function is given as:

$$\frac{\omega_m}{\omega_{ref}} = \frac{1}{\frac{J}{k_{op}}s + 1} \quad (30)$$

To verify the accuracy of the inertia quantity measured by the proposed method, experiments are done in the followings. The first experimental result is shown in Fig. 14, where the reference speed is $2000 + 500\sin(2\pi t)$. The purple line is the reference speed, and the red line is speed response. Speed1 denoted by dashed blue line is $2000 + 500/\sqrt{2}\sin(2\pi t)$, and speed2 which is the result of 45 degrees shift of speed1 denoted by dotted black line is $2000 + 500/\sqrt{2}\sin(2\pi t - \pi/4)$. These two lines are used to take a transformation from the reference speed to theory response speed (denoted by speed2). If the inertia is accurate and the PI design is reasonable, the speed response should be $2000 + 500/\sqrt{2}\sin(2\pi t - \pi/4)$. In Fig. 14, the practical speed response (the red line) agrees well with the black-dotted line, speed2.

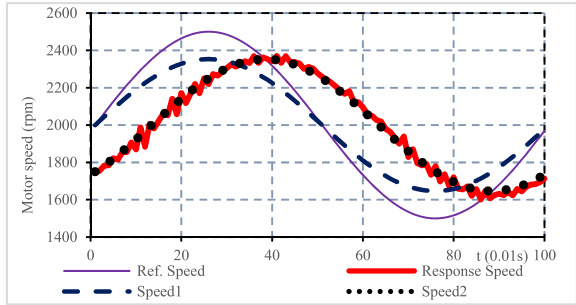


FIGURE 14. The speed response vs. referenced speed ($\omega e = 2\pi$).

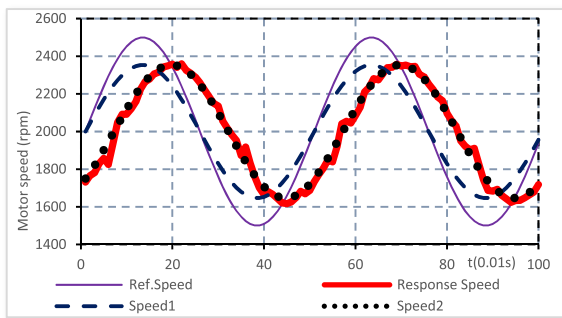


FIGURE 15. The speed response vs. referenced speed ($\omega e = 4\pi$).

When the reference signal becomes $2000 + 500\sin(4\pi t)$, the experimental result is shown in Fig. 15. Similarly, the result is accurate enough to demonstrate that the inertia

measurement method is useful and accurate. Like the experiments on inductance measuring and resistance measuring, we test many groups of speed reference signals, the method keeps a staple performance.

V. HALL POSITION SENSOR SPEED SIGNAL PROCESSING

Except the sensorless AC motor drives, most of drive systems that needs the ability of smoothly adjusting speed have a position sensor, such as a resolver, a photoelectric encoder, or a hall sensor. For a photoelectric encoder and a resolver, it's convenient to get accurate speed if the resolution is high enough. However, a hall sensor featuring with low cost is widely used in various industrial circumstances, where it cannot offer an accurate speed (Finite number of halls and long measuring period lead to the low precision of measurement), especially when the speed is varying all the time. The new inertia identification method proposed in this paper needs the amplitude of the sinusoidal speed, and hence we propose a solution to address this problem as follows.

Although there are many installation styles of hall position sensor, the signal sent into a CPU is identical as depicted in Fig. 16. The signals are three pulses with a duty of 50 percent and the phase shift angles among them is same as that of the back-EMF of a PMSM, namely 120 electrical degrees.

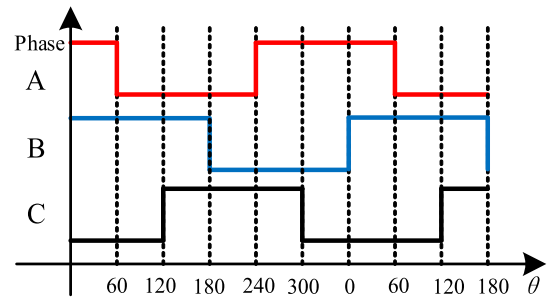


FIGURE 16. The signals from hall position sensors.

Usually, the hall signals are processed by a capture module in MCU, such as eCap module in C2000 series MCU of Texas Instrument or General Timer in STM32 or STM8S of STMicroelectronics. The operation principle is so simple, namely every rising edge or trailing edge gives an interrupt to the CPU, and the consuming time of every 60 electrical degrees can be measured using the internal CPU timer. The frequency of a general CPU is high enough to get an accurate time length of every interval of hall signals. The time between two edges can be used to acquire the mean speed of this time interval, which is a common speed computing process.

It's easy to understand that the speed gained from above method is not accurate enough, especially under the condition that the speed is always varying very fast. But if the speed is a constant number, it's accurate enough. In the aforementioned method for inertia measurement, the sinusoidal speed amplitude is very critical, and it means the common process method mentioned doesn't work in the measurement of inertia. To solve this problem, a new process way is proposed as follows.

The requirements of the measurement of friction parameter B and no-load torque T_l is satisfied using a hall position sensor, since the speed from the hall position sensor is accurate when the speed of the motor is constant. The sinusoidal characteristic of the speed and the interval time length of a constant angle are used to compute the sinusoidal speed amplitude. The detailed illustration is as follows.

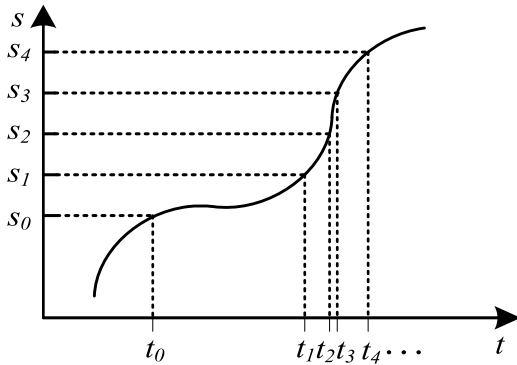


FIGURE 17. The relationship between the sampling time and motor positions.

Fig. 17 shows a diagrammatic sketch of the positions that be recorded and the interval time of every two edges. The electrical angle distance is $\pi/3$ between two edges, and the speed is given as:

$$\omega_{mdc}(t) = \frac{T_0 B}{\sqrt{B^2 + J^2 \omega^2}} \sin(\omega t - \beta) + \frac{T_{dc} - T_l}{B} \quad (31)$$

For convenience, set $(T_{dc} - T_l)/B$ as v_0 and $T_0 B / \sqrt{B^2 + J^2 \omega^2}$ as v_1 , so the speed can be written as $\omega_m = v_0 + v_1 \sin(\omega t - \beta)$.

If an integral is applied on equation (31), the position signal function can be defined as:

$$d = v_0 t - v_1 \cos(\omega t - \beta) + C \quad (32)$$

where d is the motor position and C is a constant that depends on the initial integral time. We selected three time point t_0 , t_1 , and t_2 . Therefore, the interval time length can be written as

$$\begin{aligned} d_1 - d_0 &= v_0(t_1 - t_0) - v_1 \cos(\omega t_1 - \beta) \\ &\quad + v_1 \cos(\omega t_0 - \beta) \\ d_2 - d_1 &= v_0(t_2 - t_1) - v_1 \cos(\omega t_2 - \beta) \\ &\quad + v_1 \cos(\omega t_1 - \beta) \end{aligned} \quad (33)$$

For equation (33), the left terms are the distances between two edges which is constant quantity of $\pi/3$ and can be set as Δd_1 and Δd_2 , respectively. For the right terms, $t_1 - t_0$ and $t_2 - t_1$ can be replaced by Δt_1 and Δt_2 offered by a CPU. For convenience, β can be written as $\omega(\beta/\omega)$, and $t_0 - \beta/\omega$ can be represented as t_b . Therefore, equation (33) can be rewritten as

$$\begin{aligned} \Delta d_1 &= v_0(\Delta t_1) - v_1 \cos(\omega(t_b + \Delta t_1)) + v_1 \cos(\omega t_b) \\ \Delta d_2 &= v_0(\Delta t_2) - v_1 \cos(\omega(t_b + \Delta t_1 + \Delta t_2)) \\ &\quad + v_1 \cos(\omega(t_b + \Delta t_1)) \end{aligned} \quad (34)$$

In equation (34), there are only two unknown variables, t_b and v_1 . A system with as many equations as unknowns will be consistent. First step, (34) is transformed as

$$\begin{aligned} \Delta d_1 - v_0(\Delta t_1) &= -v_1 \cos(\omega(t_b + \Delta t_1)) + v_1 \cos(\omega t_b) \\ \Delta d_2 - v_0(\Delta t_2) &= -v_1 \cos(\omega(t_b + \Delta t_1 + \Delta t_2)) \\ &\quad + v_1 \cos(\omega(t_b + \Delta t_1)) \end{aligned} \quad (35)$$

Applying the first part of equation (35), i.e., $(\Delta d_1 - v_0 \Delta t_1)$, divided by the second part, $(\Delta d_2 - v_0 \Delta t_2)$, the result can be derived as:

$$\begin{aligned} \frac{\Delta d_1 - v_0(\Delta t_1)}{\Delta d_2 - v_0(\Delta t_2)} &= \frac{-\cos(\omega(t_b + \Delta t_1)) + \cos(\omega t_b)}{-\cos(\omega(t_b + \Delta t_1 + \Delta t_2)) + \cos(\omega(t_b + \Delta t_1))} \end{aligned} \quad (36)$$

In equation (36), there is only one unknown variable t_b . Obviously, we can use the Newton-Raphson method to get this independent variable. It is simple to obtain v_1 by equation (34) with a known t_b , which should be a mean result after many experiments.

By using this method, the amplitude of the sinusoidal speed can be measured accurate for inertia identification. We have finished the experiments, and the result is considerable precise compared to the result from a photoelectric encoder.

VI. CONCLUSION

A new inertia measurement method for PMSMs is proposed in this paper. This method employs the characteristic of mechanic motion equation that performs as a first-order system. The relationship between the speed response and electromagnetic torque are used to obtain an accurate inertia result. To verify the performance of this method, an experiment using the first-order response of the cut-off frequency sinusoidal signal of the system is performed. The experiment result shows the effectiveness, robustness and accuracy of the proposed method. For a kind of special position sensor, hall sensor, an easy way to get the accurate sinusoidal speed amplitude is presented, and the experiment result is satisfying. Although this inertia measurement method is presented on a PMSM-based drive, it can almost be used in all kinds of rotating machine as long as the electromagnetic torque is controllable, and the torque response is fast enough.

REFERENCES

- [1] G. Zhang, "Speed control of two-inertia system by PI/PID control," *IEEE Trans. Ind. Electron.*, vol. 47, no. 3, pp. 603–609, Jun. 2000.
- [2] K. R. Shouse and D. G. Taylor, "A digital self-tuning tracking controller for permanent-magnet synchronous motors," *IEEE Trans. Control Syst. Technol.*, vol. 2, no. 4, pp. 412–422, Dec. 1994.
- [3] A. J. Blauch, M. Bodson, and J. Chiasson, "High-speed parameter estimation of stepper motors," *IEEE Trans. Control Syst. Technol.*, vol. 1, no. 4, pp. 270–279, Dec. 1993.
- [4] Y.-H. Kim and I.-J. Ha, "A learning approach to precision speed control of servomotors and its application to a VCR," *IEEE Trans. Control Syst. Technol.*, vol. 7, no. 4, pp. 466–477, Jul. 1999.
- [5] S. Li and Z. Liu, "Adaptive speed control for permanent-magnet synchronous motor system with variations of load inertia," *IEEE Trans. Ind. Electron.*, vol. 56, no. 8, pp. 3050–3059, Aug. 2009.

- [6] T. Senjyu, K. Kinjo, N. Urasaki, and K. Uezato, "Parameter measurement for PMSM using adaptive identification," in *Proc. IEEE Int. Symp. Ind. Electron.*, Feb. 2002, pp. 711–716.
- [7] K. Liu and Z. Q. Zhu, "Parameter estimation of PMSM for aiding PI regulator design of field oriented control," in *Proc. ICEM*, Oct. 2014, pp. 2705–2711.
- [8] *IEEE Guide for Synchronous Generator Modeling Practices and Applications in Power System Stability Analyses*, IEEE Standard 1110, 2002.
- [9] L. Sun, M. Cheng, H. Wen, and L. Song, "Motion control and performance evaluation of a magnetic-gear dual-rotor motor in hybrid powertrain," *IEEE Trans. Ind. Electron.*, vol. 64, no. 3, pp. 1863–1872, Mar. 2017.
- [10] I. Awaya, Y. Kato, I. Miyake, and M. Ito, "New motion control with inertia identification function using disturbance observer," in *Proc. Int. Conf. Ind. Electron., Control, Instrum., Automat.*, Nov. 1992, pp. 77–81.
- [11] N.-J. Kim, H.-S. Moon, and D.-S. Hyun, "Inertia identification for the speed observer of the low speed control of induction machines," *IEEE Trans. Ind. Appl.*, vol. 32, no. 6, pp. 1371–1379, Nov. 1996.
- [12] Y. Guo, L. Huang, and M. Muramatsu, "Research on inertia identification and auto-tuning of speed controller for AC servo system," in *Proc. IEEE Power Convers. Conf.-Osaka*, Apr. 2002, pp. 896–901.
- [13] S. Wang and S. Wan, "Estimations of load parameters for PMSM by MRAS," in *Proc. Int. Conf. Elect. Control Eng.*, Sep. 2011, pp. 657–660.
- [14] J.-W. Choi, S.-C. Lee, and H.-G. Kim, "Inertia identification algorithm for high-performance speed control of electric motors," *IEE Proc.-Electr. Power Appl.*, vol. 153, no. 3, pp. 379–386, May 2006.
- [15] S.-J. Hong, H.-W. Kim, and S.-K. Sul, "A novel inertia identification method for speed control of electric machine," in *Proc. IECON*, Aug. 1996, pp. 1234–1239.
- [16] F.-J. Lin and H.-M. Su, "A high-performance induction motor drive with on-line rotor time-constant estimation," *IEEE Trans. Energy Convers.*, vol. 12, no. 4, pp. 297–303, Dec. 1997.
- [17] D. Mao, J. Qiu, and C. Shi, "Identification of self-tuning induction motor drive system based on improved least-square algorithm," in *Proc. ICEM*, Oct. 2014, pp. 2545–2549.
- [18] R. Zarringhalam, A. Rezaeian, W. Melek, A. Khajepour, S. Chen, and N. Moshchuk, "A comparative study on identification of vehicle inertial parameters," in *Proc. Amer. Control Conf.*, Jun. 2012, pp. 3599–3604.
- [19] K. Liu and Z. Zhu, "Fast determination of moment of inertia of permanent magnet synchronous machine drives for design of speed loop regulator," *IEEE Trans. Control Syst. Technol.*, vol. 25, no. 5, pp. 1816–1824, Sep. 2017.
- [20] A. Khoobroo and B. Fahimi, "Magnetic flux estimation in a permanent magnet synchronous machine using field reconstruction method," *IEEE Trans. Energy Convers.*, vol. 26, no. 3, pp. 757–765, Sep. 2011.
- [21] G. Wang et al., "Self-commissioning of permanent magnet synchronous machine drives at standstill considering inverter nonlinearities," *IEEE Trans. Power Electron.*, vol. 29, no. 12, pp. 6615–6627, Dec. 2014.
- [22] K. Liu, Z. Q. Zhu, Q. Zhang, J. Zhang, and A. W. Shen, "Influence of inverter nonlinearity on parameter estimation in permanent magnet synchronous machines," in *Proc. ICEM*, Sep. 2010, pp. 1–5.
- [23] X. Sun, L. Chen, Z. Yang, and H. Zhu, "Speed-sensorless vector control of a bearingless induction motor with artificial neural network inverse speed observer," *IEEE/ASME Trans. Mechatronics*, vol. 18, no. 4, pp. 1357–1366, Aug. 2013.
- [24] X. Sun, Z. Shi, L. Chen, and Z. Yang, "Internal model control for a bearingless permanent magnet synchronous motor based on inverse system method," *IEEE Trans. Energy Convers.*, vol. 31, no. 4, pp. 1539–1548, Dec. 2016.
- [25] X. Sun, L. Chen, H. Jiang, Z. Yang, J. Chen, and W. Zhang, "High-performance control for a bearingless permanent-magnet synchronous motor using neural network inverse scheme plus internal model controllers," *IEEE Trans. Ind. Electron.*, vol. 63, no. 6, pp. 3479–3488, Jun. 2016.
- [26] X. Sun, B. Su, L. Chen, Z. Yang, X. Xu, and Z. Shi, "Precise control of a four degree-of-freedom permanent magnet biased active magnetic bearing system in a magnetically suspended direct-driven spindle using neural network inverse scheme," *Mech. Syst. Signal Process.*, vol. 88, pp. 36–48, May 2017.



KAI LIU received the B.Sc., M.Sc., and Ph.D. degrees in electrical engineering from the Harbin Institute of Technology, Harbin, in 2005, 2007, and 2014, respectively.

Since 2015, he has been with Southeast University, where he is currently a Lecturer with the School of Electrical Engineering. His teaching and research interests include the control of electrical machines and flywheel energy storage systems.



CHUANG HOU received the B.S. degree in electrical engineering from Southeast University, Nanjing, China, in 2014, and the M.S. degree in electrical engineering from the School of Electrical and Electronic Engineering, Nanjing, in 2017.

His research interests include power converters, ac motor drives with applied modern control theories, and digital controller using the digital signal processor implementations.



WEI HUA (M'03–SM'16) received the B.Sc. degree in electrical engineering from the Department of Electrical Engineering, Southeast University, Nanjing, China, in 2001, and the Ph.D. degree in electrical engineering from the School of Electrical and Electronic Engineering, Nanjing, in 2007.

Since 2007, he has been with Southeast University, where he is currently a Professor with the School of Electrical Engineering. His teaching and research interests include the design, analysis, and control of electrical machines, especially for brushless machines, and motor drives for electric vehicles. He has authored or co-authored over 150 technical papers and holds over 50 patents in these areas.

• • •